Biochimica et Biophysica Acta 1798 (2010) 202–209

Contents lists available at ScienceDirect

Biochimica et Biophysica Acta

journal homepage: www.elsevier.com/locate/bbamem

A solid-state NMR study of changes in lipid phase induced by membrane-fusogenic LV-peptides

Prashant Agrawal [a,1], Suzanne Kiihne [a], Johan Hollander [a], Mathias Hofmann [b], Dieter Langosch [b], Huub de Groot [a,*]

[a] Biophysical Organic Chemistry/Solid State NMR, LIC, Leiden University, Einsteinweg 55, 2333 CC Leiden, The Netherlands
[b] Lehrstuhl Chemie der Biopolymere, TUM, Weihenstephaner Berg 3, 85354 Freising, Germany

ARTICLE INFO

Article history:
Received 14 April 2009
Received in revised form 15 October 2009
Accepted 25 October 2009
Available online 30 October 2009

Keywords:
Membrane fusion
Transmembrane fusogenic polypeptide
^{31}P solid state NMR

ABSTRACT

Membrane fusion requires restructuring of lipid bilayers mediated by fusogenic membrane proteins. Peptides that correspond to natural transmembrane sequences or that have been designed to mimic them, such as low-complexity "Leu-Val" (LV) peptide sequences, can drive membrane fusion, presumably by disturbing the lipid bilayer structure. Here, we assess how peptides of different fusogenicity affect membrane structure using solid state NMR techniques. We find that the more fusogenic variants induce an unaligned lipid phase component and a large degree of phase separation as observed in ^{31}P 2D spectra. The data support the idea that fusogenic peptides accumulate PE in a non-bilayer phase which may be critical for the induction of fusion.

1. Introduction

Membrane fusion implies that two phospholipid bilayers are merging in an aqueous environment. Fusion can be triggered by a variety of integral membrane proteins such as SNAREs and viral fusion proteins [1–3]. The TMSs of these proteins play a direct role in fusion as indicated by recent *in vivo* studies [4–6]. In addition, *in vitro* studies show that membrane-embedded synthetic TMS-peptides with low-complexity LV peptide sequences that mimic the natural system can drive liposome–liposome fusion depending on the structural flexibility of their secondary structure [7–9]. Thus, LV-peptides represent a simplified system to study the minimal requirements for fusion.

During fusion, major rearrangements of lipid structures occur in a confined region of interbilayer contact. Lipid composition affects the various steps in fusion from outer leaflet mixing to inner leaflet mixing and fusion pore formation. This is strongly correlated with their geometrical shape. For example, phosphatidylethanolamine is cone-shaped due to its small head-group and thus favors formation of negative membrane curvature that is associated with hemifusion, i.e. outer but not inner leaflet mixing [10–14]. Solid state NMR is a powerful tool for determining the structure and dynamics of membranes and their interaction with proteins or peptides. In particular, the microscopic phase properties of membranes can be investigated by ^{31}P solid state NMR [11]. Oriented bilayers can be prepared from a variety of lipid mixtures to mimic specific biomembranes, including bacterial, mammalian and myelin cell membranes [15,16]. By using macroscopically oriented membranes, which have much better resolved ^{31}P resonances than unoriented powder samples, lipid domains with different mobilities and morphologies can be distinguished. The spectral line shapes of proton-decoupled ^{31}P spectra of phospholipid membranes have been used to analyze the orientational order of the phospholipid head group [17].

Recent studies on membrane fusion provide useful insight into the sequence requirements of LV-peptides but they did not address the interaction of peptides with lipids [7]. To investigate this, we take a direct approach and study the impact of different LV-peptides listed in Table 1 on membrane structure [7]. All peptides have a central hydrophobic core, consisting of Leu, Val, and in one case a Gly–Pro pair. Each peptide is flanked on either side by 3 Lys and contains one Trp residue for quantification [18]. Sequence composition reflects the design principle, which is based on the different conformational preferences of the hydrophobic residues. While Leu stabilizes the helical state, substituting Leu for Val decreases helix stability in isotropic solution and favors β-sheet formation. A central Gly–Pro pair

Abbreviations: DOPS, 1,2-dioleoyl-sn-glycero-3-[phospho-L-serine]; DOPE, 1,2-dioleoyl-sn-glycero-3-phosphoethanolamine; HBTU, [2-(1 H-benzotriazol-1-yl)-1,1,3,3- etramethyluronium hexafuorophosphate]; NBD-PE, N-(7-nitro-2,1,3-benzoxadiazol-4-yl)hexadecylphosphatidylethanolamine; NMP, N-methylpyrrolidinone; POPC, 1-palmitoyl-2-oleoyl-sn-glycero-3-phosphocholine; Rh-PE, N-(lissamine rhodamin B sulfonyl)hexadecylphosphatidyl-ethanolamine; PC, phosphatidylcholine; PE, phosphatidylethanolamine; PS, phospatidylserine; SNARE, soluble NSF (N-ethylmaleimide-sensitive factor) attachment protein receptor; TMS, transmembrane segments; TIS, triisopropyl silane

* Corresponding author.
E-mail address: groot_h@lic.leidenuniv.nl (H. de Groot).
[1] Current address: Biomedical NMR, Department of Biomedical Engineering, Eindhoven University of Technology, P.O. Box 513, 5600 MB Eindhoven, The Netherlands.

0005-2736/$ – see front matter © 2009 Elsevier B.V. All rights reserved.
doi:10.1016/j.bbamem.2009.10.015

Table 1
Two sets of peptides are used in this study.

Set 1: length dependency	
LV12	K K K W **L V L V L V L V L V L V** K K K
LV16	K K K W **L V L V L V L V L V L V L V L V** K K K
LV20	K K K W **L V L V L V L V L V L V L V L V L V L V** K K K
LV24	K K K W **L V L V L V L V L V L V L V L V L V L V L V L V** K K K
Set 2: L/V ratio	
L16	K K K W **L L L L L L L L L L L L L L L L** K K K
LV16	K K K W **L V L V L V L V L V L V L V L V** K K K
LLV16	K K K W **L L V L L V L L V L L V L L V L** K K K
LV16G8P9	K K K W **L V L V L V L G P V L V L V L V** K K K

Set 1 comprises the peptides with lengths between 19 residues and 31 residues. Set 2 consists of peptides with the same hydrophobic length and different composition of the inner hydrophobic core.

destabilizes the helical state further [19]. In liposomal membranes, the aliphatic peptides (L16, LLV16, LV16) are largely helical while LV16G8P9 assumes a predominant β-sheet structure with a strong turn component [19,20]. Moreover, recording deuterium/hydrogen-exchange kinetics revealed that the conformational dynamics of the peptide backbones increases with an increasing Val/Leu ratio and introduction of the Gly–Pro pair [9].

A principle advantage of ^{31}P NMR studies is in the similarity of the conditions used for sample preparation with the functional fusion assays, as we use a synthetic lipid mixture mimicking the natural system. In addition, our previous solid state NMR studies on mechanically aligned bilayers made up of a biomimetic three-lipid mixture already showed that a strong perturbation of the lipid bilayer can be induced by a small fraction of LV16G8P9, which suggests that this is an important marker for fusogenic peptide behavior [20].

It has been proposed in the past that during the membrane fusion process lipids go through various lipid phases [17]. The data presented here demonstrate that small amounts of peptide can give rise to pronounced macroscopic lipid rearrangements. This indicates that the interactions between hydrophobic sequences and the phospholipid bilayers can have remarkably strong control over the suprastructure of a multilamellar system.

2. Materials and methods

POPC, DOPS and DOPE were purchased from Avanti Polar Lipids, Birmingham, AL. Peptides were either synthesized according to the procedures published before or commercially obtained from PSL, Heidelberg, Germany, and purified to >90% by high-performance liquid chromatography [7,20]. Purities were determined by mass spectrometry. Concentrations of peptide solutions were determined via tryptophan absorbance at 282 nm in a 1:1 (v/v) mixture of trifluoroethanol and dimethyl sulfoxide using an extinction coefficient of 5600 M^{-1} cm^{-1}.

Liposome preparation, fusion assays and quantification of the peptide/lipid ratios were done as described previously [21]. Briefly, liposomes with or without TMS-peptides were prepared from mixtures of egg PC /brain PE /brain PS at a ratio of 3:1:1 (w/w/w) with or without 0.8% (w/w) of NBD-PE and Rh-PE (Molecular Probes) by sonication in fusion buffer (25 mM Tris–HCl, pH 7.4, 150 mM NaCl, 0.1 mM EDTA, 5 mM DTT). Fusion assays were performed using the fluorescence dequenching method [22] using "donor" liposomes containing fluorescence labels and unlabeled "acceptor" liposomes (2.5 mg/ml phospholipid) at a ratio of 1:4 (v/v). The peptide-independent, spontaneous fusion of pure liposomes was routinely determined in parallel and subtracted from the values obtained with peptide-containing liposomes.

Samples for solid-state NMR studies were prepared by dissolving POPC, DOPE and DOPS in chloroform in a 3:1:1 ratio. The overall lipid composition was kept constant, which restrains the sample variation. A peptide dissolved in trifluoroethanol was added in a 1:100, peptide/lipid molar ratio. The mixture was vortexed and was applied onto 15 ultra thin cover glasses (6.2×20 mm; Paul Marienfeld GmbH and Co. KG, Lauda-Konigshofen, Germany), first dried under a stream of nitrogen, and kept overnight in high vacuum. Subsequently, the plates were hydrated by spraying with fusion buffer containing 150 mM NaCl, 20 mM Tris, and 0.2 mM EDTA (pH 7.4). The plates with peptide–lipid films were equilibrated at 4°C for 72 h and then stacked on top of each other. The stacks were stabilized at 4°C for 6 h and sealed with Teflon tape and plastic wrappings to prevent dehydration from RF induced heating [18].

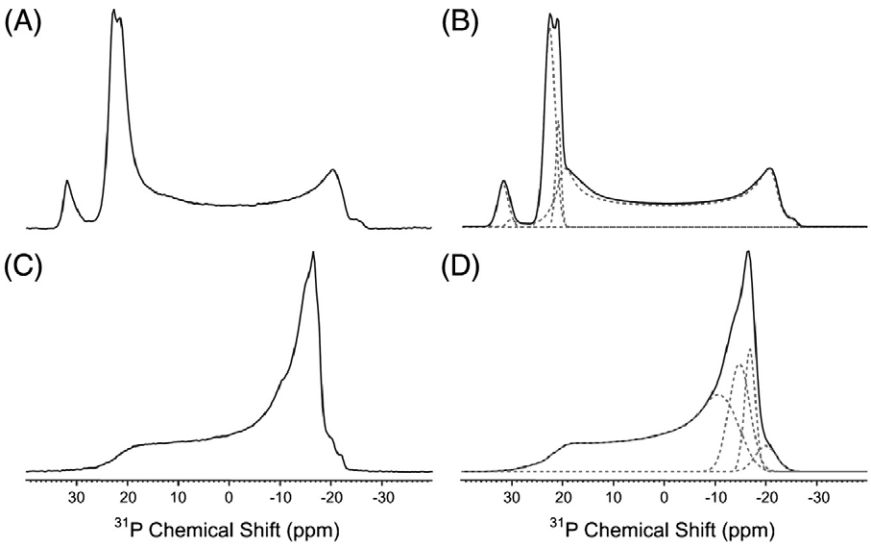

Fig. 1. ^{31}P spectra of oriented peptide-free bilayer samples, with the bilayer normal parallel (A and B) or perpendicular to the magnetic field (C and D). The data were recorded at 310 K and 7.4 pH with 6 K scans. The simulated spectra are shown in B and D, and are generated by calculating the responses of various lipid species, shown as dotted lines. (A and B) For the lipid mixture spectrum the aligned bilayer component representing ordered lipid molecules has a composition PC:PE:PS ~24:7:5 and the cylindrical type response has a composition PC:PE:PS ~36:13:15 (as inferred from the composition of the aligned phase and the relative amount of each lipid species used in the sample, at a ratio of 60% POPC, 20% DOPS and 20% DOPE). (C) ^{31}P spectrum of the oriented lipid mixture, with the bilayer normal perpendicular to the magnetic field B_0. (D) The simulated spectrum is generated by calculating the responses of various lipid species, shown as dotted lines.

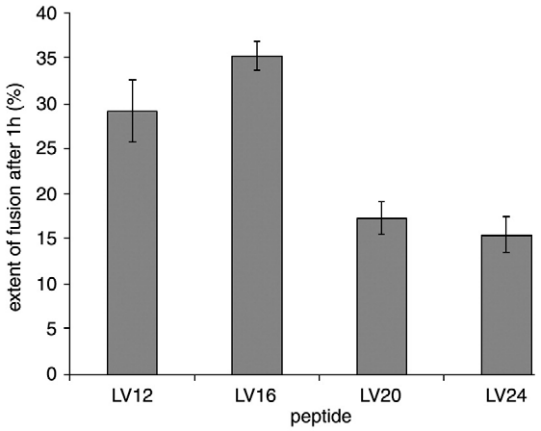

Fig. 2. Fusogenic activity of peptides of different hydrophobic length. The extents of fusion as recorded after 1 h of incubation at a molar peptide/lipid ratio of 0.005 depend on the length of the LV core sequence.

The samples were inserted into a multichannel flat coil probe head and placed in a Bruker AV750 spectrometer with the membrane normal oriented parallel to the magnetic field direction. Proton-decoupled ^{31}P solid-state NMR 1D spectra were recorded using a Hahn echo pulse sequence with a 90° pulse length of 7.8 μs, an echo delay of 40 μs, 6 K scans of 1 K data points with a spectral width of 94.339 kHz, and a recycle delay of 3 s [23]. For the oriented lipid mixture without peptide, a sample ^{31}P 1D spectrum was recorded with the alignment axis at 90°, i.e. perpendicular to the magnetic field direction. A line broadening of 10 Hz was applied before Fourier transformation. The spectra were processed without first order phase correction and calibrated to $(NH_4)_2HPO_4$ at 0 ppm chemical shift. The NMR measurements were performed using similar conditions of pH 7.4, at a temperature of 310 K and with ~30 min of equilibration time in the spectrometer before recording the data. Spectra were collected over 30-min intervals to monitor changes. Proton-decoupled ^{31}P-^{31}P 2D NOESY solid-state NMR spectra were recorded using various mixing times τ_m, ranging from 250 ms to 500 ms and with an acquisition time of 12 h. All observations were confirmed by measuring duplicate samples.

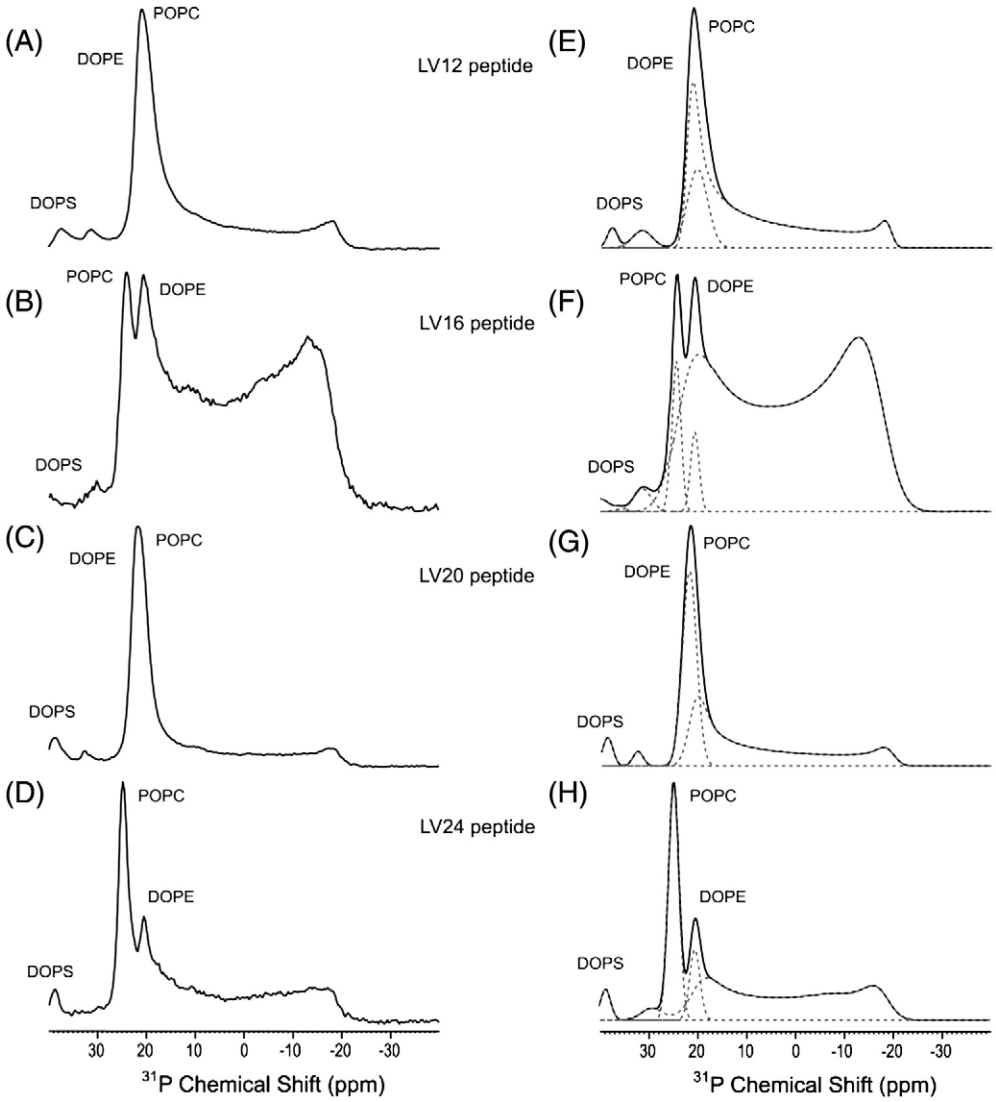

Fig. 3. ^{31}P spectra of oriented bilayer samples loaded with peptides of different hydrophobic length and with the bilayer normal parallel to the B_0 are shown in the left panel. The right panel contains the simulated spectra that are generated by calculating the responses of various lipid species, shown as dotted lines. The spectrum for the lipid mixture loaded with non-fusogenic peptide LV12 is shown in (A), while (B) shows the data for the lipid mixture containing the fusogenic peptide LV16. Spectra of lipid mixtures with non-fusogenic peptides LV20 or LV24 are shown in (C) and (D), respectively.

3. Results and discussion

The aim of the studies in this article is to address the effect of LV-peptides on the structure of a biomimetic lipid membrane. The predominant phospholipids in synaptic vesicles are PC, PE and PS that collectively comprise ~70% of all phospholipids [24]. A mixture of PE, PS, and PC in a 1:1:3 ratio is thus used here to simulate the biological membrane composition of synaptic vesicles [25]. The impact of the peptides is studied at peptide to lipid ratios of 1:100 using different solid-state NMR techniques.

The ^{31}P NMR line shape of the biomimetic pure three-lipid mixture in fusion buffer is dominated by signals that are characteristic for oriented and unoriented phospholipid bilayers (Fig. 1A) [18]. Three narrow signals at 21.3 ppm, 22.5 ppm, and 32 ppm are assigned to 0° oriented PC, PE, and PS in the bilayer phase, respectively, by comparison with values known for the pure lipids [4–6]. The broad signal at –20 ppm and the shoulder at −24 ppm reveal cylindrical type lipid arrangements in the unoriented phase, with the long axis of the cylinder perpendicular to the field [25]. Fig. 1B illustrates how the relative fractions can be estimated using simulated curves generated for the various lipid phases [11,26]. For the aligned region PC:PE:PS ~24:7:5, leading to a PC:PE:PS ~36:13:15 ratio in the lipid cylinder phase [27]. For the pure lipid mixture there is a significant difference in lipid composition between the two fractions (Fig. 1A). The aligned bilayer phase has a composition of ~34% of total lipids, while on the other hand the unoriented high curvature phase consists of ~64% of the lipids similar to the composition of the natural lipid mixture. Fig. 1C shows the spectrum of the biomimetic lipid mixture at 90° orientation. To confirm that the −20 ppm signal in the spectrum does not have residual anisotropy, the ^{31}P spectra of the same samples rotated by 90° with the glass plate normal perpendicular to B_0 were measured (Fig. 1C). The corresponding simulation is shown in Fig. 1D. The narrow signals represent ~35% of the lipids while the broad signal comprises ~65% of the lipids and reflects a cylindrical type component with a small presence of vesicle type distribution.

The LV-peptides are divided into two classes; one is based on the length of the hydrophobic core and the other class has a different composition within the hydrophobic core. In the first set, the hydrophobic core is comprised of alternate Leu and Val and its length varies between 12 residues in the LV12 peptide to 24 residues in the LV24 peptide (Table 1, Set 1). This variation in length can provide insight into the effect of the length of the hydrophobic part of peptides on fusogenicity. In the second set of peptides, the primary structure is varied such as to change the conformational flexibility of the hydrophobic core (Table 1, Set 2) [7,9,18,19].

The peptides with varying core length were first studied for fusogenic activity by standard fluorescence dequenching assays in the POPC/DOPE/DOPS (3/1/1) mixture which is also used for the NMR experiments [18]. This assay is based upon fluorescence resonance energy transfer from NBD-PE to Rh-PE present at quenching concentrations in donor liposomes. Upon fusion of labeled with unlabeled liposomes the average distance between the fluorophores, and thus NBD fluorescence, increases over time and this is taken as a measure of fusion. Fig. 2 compares the membrane fusogenicity of different peptides at a molar peptide/lipid ratio of 0.005. The extent of fusion seen after 1 h follows the rank order: LV16>LV12>>LV20≈LV24. Thus, hydrophobic length appears critical for fusion.

Oriented bilayers show reproducible changes upon incorporation of peptides with different lengths (Fig. 3). After addition of peptides LV12 and LV20, the 0° orientation signal of the POPC response shifts to σ =~21 ppm and is superimposed on the DOPE response. For LV24, the POPC signal shifts to 25.11 ppm with a DOPE component resonating with σ ≈20.86 ppm. In addition, a weak DOPS signal as observed at 32 ppm for the pure lipid bilayer (Fig. 1A) shifts to ~38 ppm upon loading with LV24 and for LV12 it shifts to ~31.4 ppm (Fig. 3A and D). The broad signal at ~−18 ppm is less intense than for the pure lipid system, indicating a stabilization of the aligned phase and a signal characteristic of a toroidal pore type component for LV12 and LV20 samples. For LV24 the broad signal that peaks at −18 ppm reflects a cylindrical distribution in the unoriented phase, which comprises ~60% of the lipids (Figs. 3H and 4). The data for the LV24 sample can be simulated with signal ratios PC:PE:PS ~7:2:1 for the aligned region and PC:PE:PS ~8:3:4 for the unoriented region (Figs. 3H and 4). In case of LV12 the relative intensities of PC:PE:PS are ~10:2:1 in the aligned region, while the toroidal pore type fraction represents ~74% of the lipids with relative intensities PC:PE:PS ~5:2:2 (Figs. 3E and 4). On the other hand LV20 has PC:PE:PS

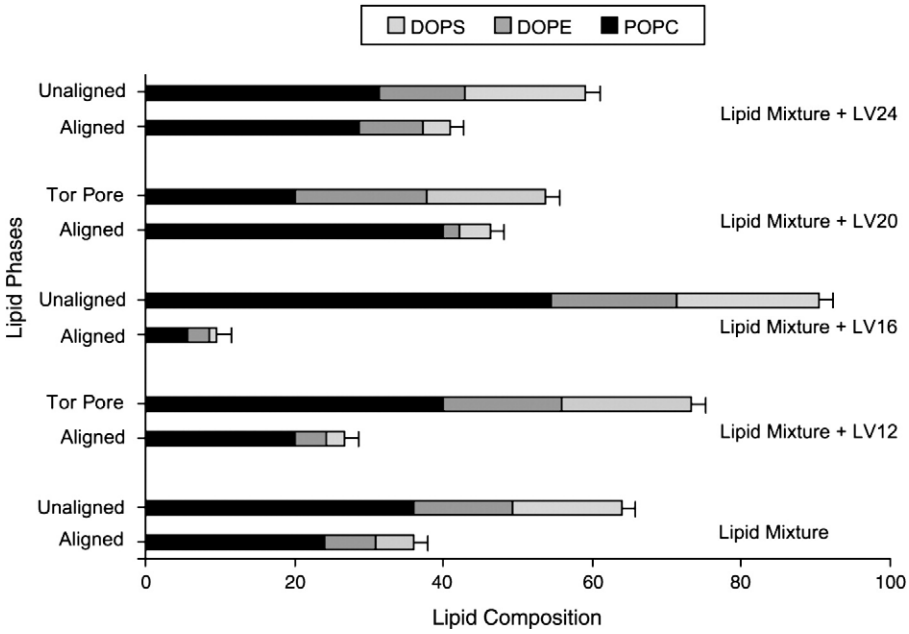

Fig. 4. The compositions of PC, PE and PS in the two phases in a lipid mixture without peptide and in the lipid mixture containing peptides LV12, LV20, LV16, or LV24 (1 mol %). The error bars are based on estimates for the lipid compositions of two independently prepared samples.

~20:1:2 in the aligned region and ~54% of lipids in the toroidal pore type lipid component with the PC:PE:PS in a ~5:4:4 ratio (Figs. 3G and 4).

When the most fusogenic peptide LV16 is incorporated in the lipid bilayer the 0° orientation signal of DOPE is shifted to $\sigma \approx 20.6$ ppm with a POPC component resonating with $\sigma \approx 24.08$ ppm (Fig. 3B). Here the high curvature phase has a significant component reflecting an isotropic distribution of lipid molecules, ~11% perturbing the predominant symmetric cylinder line shape (Fig. 3F). There is also vesicle type component that may correspond to an increased fraction of end lipids cupping hydrophobic edges of a bilayer. This suggests that cylindrical structures can become more vesicle-type in the presence of a fusogenic peptide (Fig. 3F). It is clear that LV16 stabilizes the high curvature phase relative to the flat bilayer phase. The data are simulated with relative intensities PC:PE:PS ~6:3:1 for the flat membrane fraction and PC:PE:PS ~3:1:1 for the high curvature component (Figs. 3F and 4).

As shown previously, the fusogenicity depends on the sequence of the hydrophobic core (Table 1, Set 2) [28,29]. A Leu-based peptide (L16) is virtually non-fusogenic, while mixing Leu and Val residues yields intermediate (LLV16) to strong (LV16) fusogenic activity [7]. Placing a Gly/Pro pair in the middle of the hydrophobic core of LV16 (LV16-G8P9) significantly enhances fusion. Accordingly, fusion extents increase in the following order: L16<LLV16<LV16<LV16G8P9 [7].

These peptides were incorporated in oriented bilayers and the ^{31}P lipid signals changes were monitored (Fig. 5). After addition of LLV16 a toroidal pore type signal forms, representing ~52% of the lipids with relative intensities PC:PE:PS ~1:1:1, while the aligned region has relative intensities PC:PE:PS ~21:1:2 (Figs. 5B, F and Fig. 6). The POPC 0° orientation signal resonates with $\sigma =$ ~21.33 ppm, and is superimposed on a DOPE response (Fig. 5B). For the L16, the broad signal that peaks at 21 ppm and −18 ppm reflects a cylindrical distribution in the unaligned phase and comprises ~60% of the ^{31}P signal (Figs. 5E and 6). The data for the aligned region can be simulated with a signal ratio PC:PE:PS ~9:3:1 and PC:PE:PS ~11:3:6 for the unaligned region (Figs. 5E and 6).

When the lipid mixture is loaded with fusogenic LV16G8P9 peptide, the 0° oriented signal of a PC component resonates with $\sigma \approx 24.5$ ppm while the PE response is shifted to $\sigma \approx 19.5$ ppm. The high curvature phase also comprises a significant fraction of vesicle

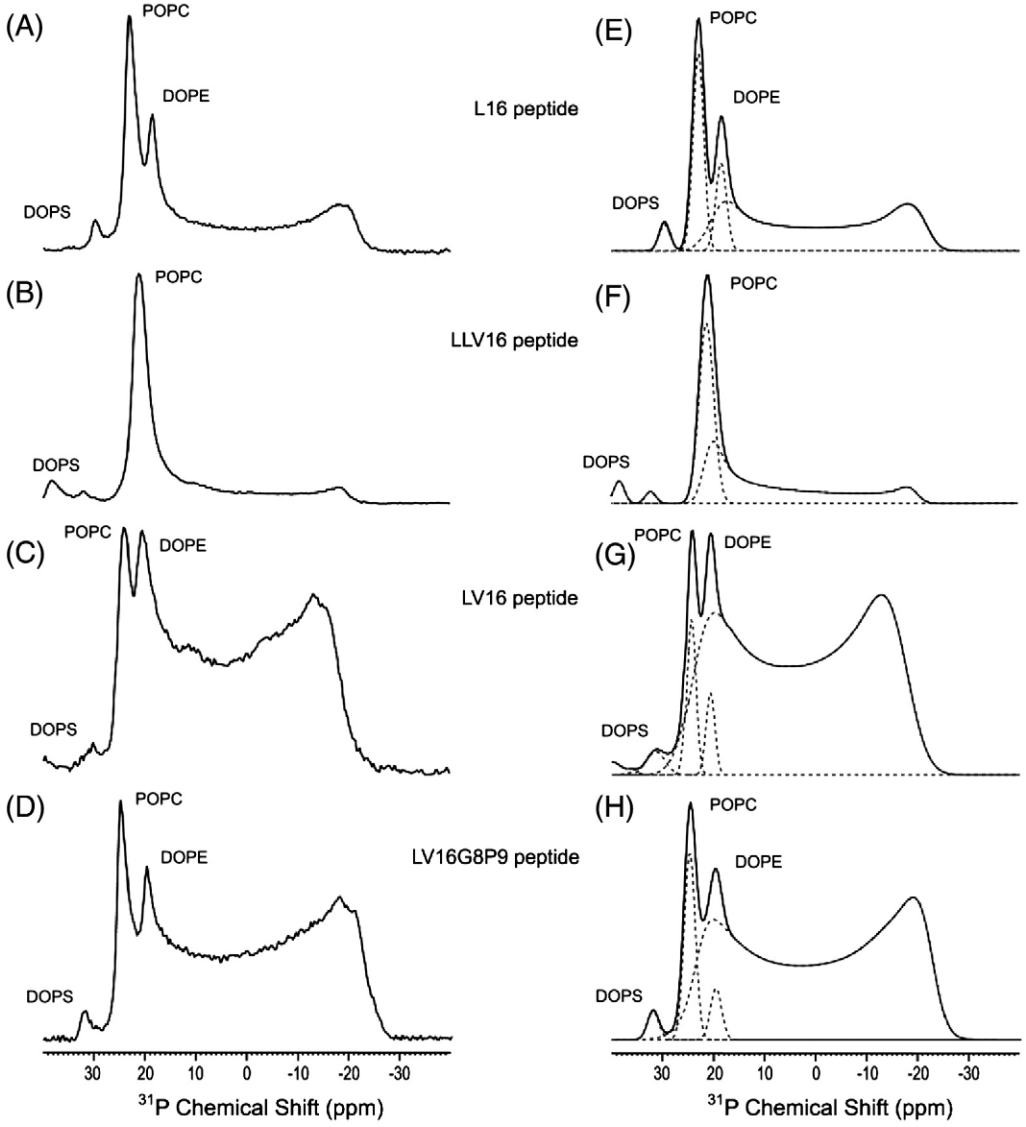

Fig. 5. ^{31}P spectra of oriented bilayer samples, with the bilayer normal parallel to the B_0 are shown in left panel. The simulated spectra generated by calculating the responses of various lipid species, shown as dotted lines, are shown in the right panel. (A) Spectrum for the lipid mixture with the non-fusogenic peptide L16. (B) Spectrum for the lipid mixture with the low-fusogenic peptide LLV16. (C) Lipid mixture with the fusogenic peptide LV16. (D) Lipid mixture with the most fusogenic peptide LV16G8P9. The data were recorded with 6 K scans at 310 K and pH 7.4.

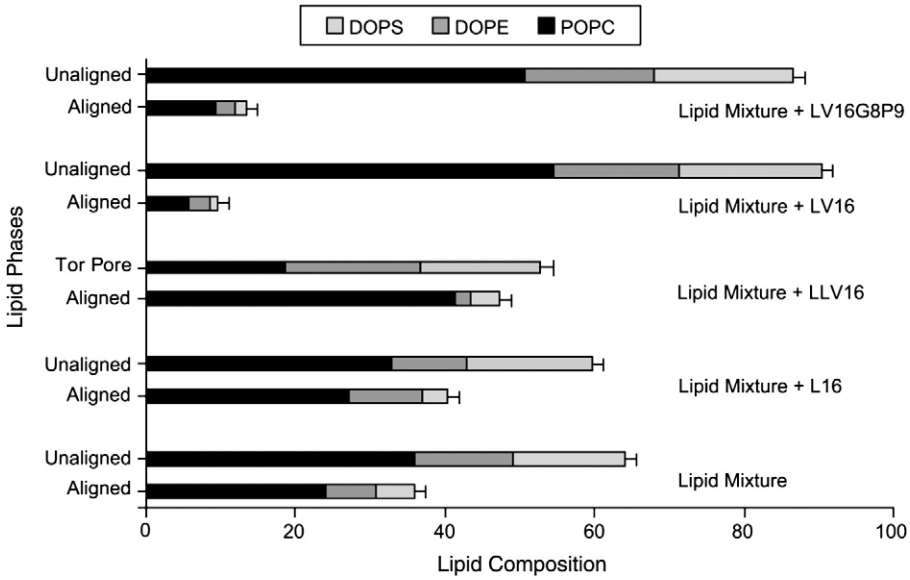

Fig. 6. Graphical representation of the PC, PE and PS composition of the biomimetic lipid mixture without and with the various peptide (1 mol%) in two different phases. The error bars are based on estimates for the lipid compositions of two independently prepared samples.

type signal, ~16%, which is reflected by an anisotropic response in the signal with $\sigma \approx 24$ ppm and $\sigma_{\perp} \approx -18$ ppm, perturbing the symmetric cylinder line shape (Fig. 5H). It is clear that LV16G8P9 stabilizes the enhanced curvature phase relative to the flat bilayer phase [19].

When the sample with LV16G8P9 is monitored over an extended time period, additional changes are observed (Fig. 7). After 3 weeks, a single oriented bilayer response with $\sigma \approx 23$ ppm is observed that represents ~7% of the lipids, mainly POPC (Fig. 7H). In addition, a pronounced anisotropic signal is present in the center of the spectrum with a broad maximum at $\sigma^{H} \approx 3$ ppm and with $\sigma_{\perp}^{H} \approx -18$ ppm. A minor shoulder at $\sigma^{H} \approx 8.6$ ppm can be attributed to DOPS (Fig. 7H). The broad signal comprises the response from essentially all DOPE and DOPS. It reveals a large fraction of unoriented hexagonal tubes, which can be attributed to DOPS and accounts for ~31% of the total NMR signal. The resonance line shape of the remainder of the lipids, ~62%, still has cylindrical character and consists of ~50% POPC and ~12% DOPS and DOPE. Although the fitting done for these spectra has considerable error margins it allows to estimate the composition. The broadening of the aligned signals has been attributed in the past to wobbling of headgroups and increased mobility [30].

To determine if the different lipid phases in lipid membranes containing LV16G8P9 are spatially separated or not, 2D ^{31}P exchange experiments were performed (Fig. 8). Lipids undergo lateral diffusion with diffusion coefficients of 10^{-7} to 10^{-8} cm^2/s [28,29]. If the isotropic lipids are contiguous with the residual oriented lipids, and if a characteristic radius of curvature of ~1 μm is assumed for the membrane, then lipid reorientation induced by lateral diffusion is expected to change the ^{31}P frequency on time scales of 10–100 ms. This should give rise to cross-peaks in the 2D exchange spectra. Fig. 8 displays 2D ^{31}P spectra of the lipid mixture containing the LV16G8P9 peptide, acquired with mixing times of 250 ms, 400 ms and 500 ms. Even at this longer mixing time only weak cross peaks between the 0° and the 90° peak are observed, despite their strong diagonal intensities. This confirms that the domains corresponding with the unaligned lipid phase are spatially well separated from the lamellar fraction.

Our current results reveal that LV-peptides can profoundly alter the lipid phase of an oriented bilayer depending on their fusogenicity. In one set of peptides, the length of the hydrophobic core is held constant and fusogenicity has previously been shown to increase in the order L16<LLV16<LV16<LV16G9P9 [7]. Interestingly, only the more fusogenic TMDs, LV16 and LV16G8P9, significantly increased the fraction of unaligned lipids. In addition, for the LV16 and LV16G8P9, the oriented peaks are broad, indicating the wobbling of lipid headgroups and increased mobility. The effects seen with both peptides differed from each other in that the peak of the unaligned phase at +20 ppm is shifted to +12 ppm only with LV16, indicating a different microenvironment of the lipid phosphates surrounding the latter TMD. This different behavior of the lipids parallels the different secondary structures of the peptides in membranes seen previously. While LV16 is largely α-helical in liposomes, LV16G8P9 adopts mostly β-sheet [19]. The lack of exchange between the lamellar and nonlamellar phases that was deduced from the NOESY spectra is well in line with data collected from lipid membranes without any peptides (data not shown) and confirms a spatial separation of lamellar and nonlamellar lipids.

With the second set of peptides investigated here, the lengths of the hydrophobic core were varied between 12 and 24 residues. Fusion assays revealed strong fusogenicities for LV12 and LV16. Despite its significant fusogenicity, LV12 did not induce formation of unaligned lipid phase to the extent seen with LV16. This is not as surprising as it may seem at first glance since LV12 folds mainly as β-sheet that is accompanied by a minor fraction of α-helix in the membrane (B. Poschner and D.L., manuscript in revision). This may indicate that LV12 induces fusion by a mechanism that does not involve the major changes in lipid phase seen after incorporating LV16. At the same time, this would imply that the β-sheet structures seen with LV12 and LV16G8P9 in the membrane differ from each other. Indeed, LV16G8P9 has been proposed to form a β-hairpin at the site of the Gly–Pro pair on the basis of a significant amount of observed β-turn structure [19], which is not expected for LV12.

Curve fitting with lipid model spectra reveals that L16, LV16, LV24, and LV16G8P9 may induce cylindrical phase to different extents while the spectra seen after incorporation of LV12, LV20, and LLV16 are reminiscent of a toroidal pore. Cylindrical phase may correspond to local sites of fusion between the apposed bilayers in the membrane stack. Local fusion may generate half-cylinders of bilayers whose spectrum adds up to the one known for an actual cylinder. Toroidal pores have not been associated yet with the actual sites of fusion. Rather, lipid pores have been implicated to form adjacent to hemifusion diaphragms by molecular dynamics simulations [31,32] and self-consistent field theory [33]. These pores have

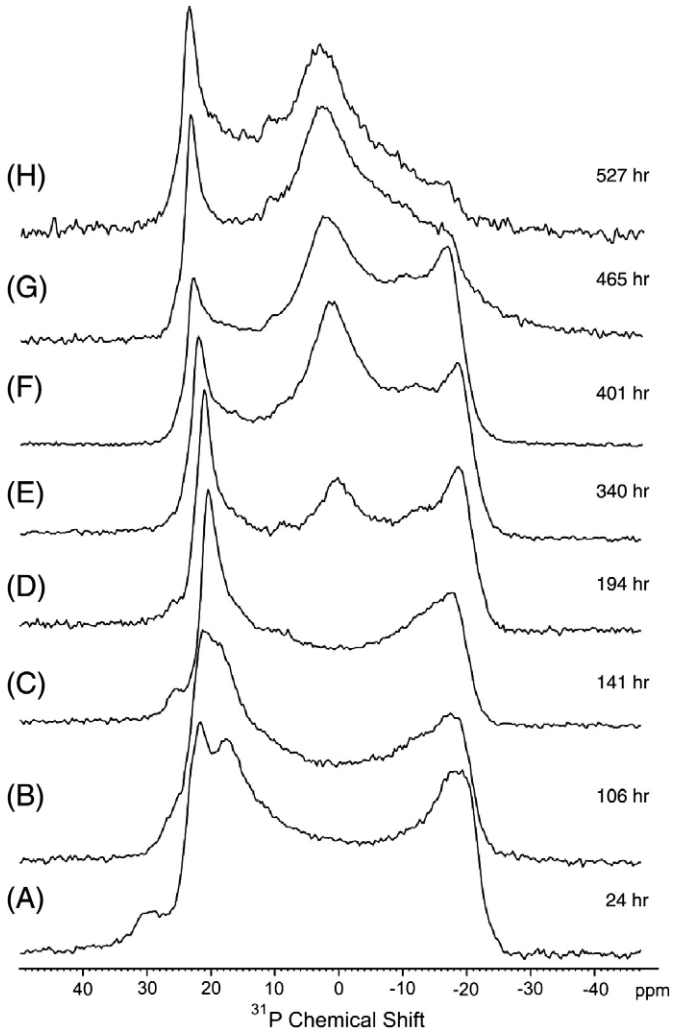

Fig. 7. Lipid phase changes induced by LV16G8P9 as a function of time. Proton-decoupled Hahn-echo ^{31}P 1D solid-state NMR spectra of the POPC:DOPE:DOPS = 3:1:1 lipid mixture loaded with the fusogenic peptide LV16G8P9. The data were recorded at 310 K and pH 7.4 in 6 K scans with the bilayer normal parallel to the magnetic field. Spectra were recorded over an extended period up to 3 weeks to monitor the long-term changes in the biomimetic lipid mixture after addition of the fusogenic peptide.

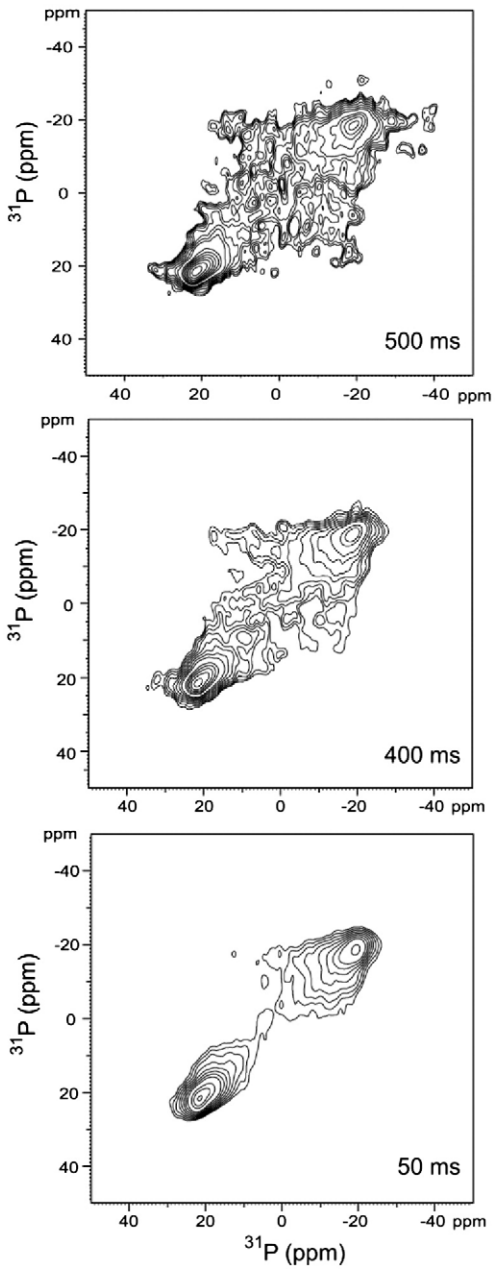

Fig. 8. 2D ^{31}P exchange NOESY solid-state NMR spectra of oriented lipid membranes with 1% LV16G8P9. The exchange mixing times are 250, 400 and 500 ms. The spectra are recorded at 310 K and pH 7.4 with a total acquisition time of 12 h.

been proposed to mediate transfer of lipid molecules from the outer to the inner the monolayers at a stage between stalk formation and full fusion.

Another remarkable observation made in the current study is that the unaligned phase is enriched in PE and PS, which may be connected with a requirement for negative-curvature lipids for stalk formation. It is thought that cone-shaped lipids like PE favor the formation of stalks by stabilizing negative curvature of the outer leaflet [30]. Indeed, imaging studies on *Tetrahymena* mating cells have shown that membrane fusion sites probably contain a large quantity of cone-shaped lipids such as PE [34]. Consequently, the more fusogenic peptides may efficiently concentrate negative-curvature lipids to sites from which stalk formation may occur as a prelude to fusion.

Finally, when a sample containing LV16G8P9 is measured over an extended period of time, a pronounced phase change of the lipids is observed in a few weeks. The appearance of an anisotropic response reveals the presence of unoriented hexagonal tubes due to relaxation of strain at a much longer time scale. This is not observed for the lipid mixture without peptide and the lipid mixture containing the non-fusogenic L16 (data not shown). A hexagonal pattern is very characteristic since it requires partial averaging of the chemical shift by rapid self-diffusion over the radius of the tubes. The normal and inverted hexagonal phase cannot be distinguished using ^{31}P NMR because they have the same symmetry. Over time, lipid separation proceeds and the system will reach equilibrium. The equilibration time is reduced by peptides that facilitate domains of high curvature.

Acknowledgements

We thank Bernhard Poschner for help with preparation of Fig. 2. Financial support for this work is received from the Volkswagen-stiftung Conformational Control of Biomolecular Function Funding Initiative. The 750 MHz equipment was financed in part by demonstration project BIO4-CT97-2101 of the commission of the European Communities.

References

[1] R. Jahn, T. Lang, T.C. Sudhof, Membrane fusion, Cell 112 (2003) 519–533.
[2] C. Peters, M.J. Bayer, S. Bühler, J.S. Andersen, M. Mann, A. Mayer, *Trans*-complex formation by proteolipid channels in the terminal phase of membrane fusion, Nature 409 (2001) 581–588.
[3] R. Blumenthal, M.J. Clague, S.R. Durell, R.M. Epand, Membrane fusion, Chem. Rev. 103 (2003) 53–69.
[4] J. Rohde, L. Dietrich, D. Langosch, C. Ungermann, The transmembrane domain of Vam3 affects the composition of cis- and trans-SNARE complexes to promote homotypic vacuole fusion, J. Biol. Chem. 278 (2003) 1656–1662.
[5] C.G. Schuette, K. Hatsuzawa, M. Margittai, A. Stein, D. Riedel, P. Kuster, M. Konig, C. Seidel, R. Jahn, Determinants of liposome fusion mediated by synaptic SNARE proteins, Proc. Natl. Acad. Sci. U. S. A. 101 (2004) 2858–2863.
[6] D. Langosch, B. Brosig, R. Pipkorn, Peptide mimics of the vesicular stomatitis virus G-protein transmembrane segment drive membrane fusion in vitro, J. Biol. Chem. 276 (2001) 32016–32021.
[7] M. Hofmann, K. Weise, J. Ollesch, P. Agrawal, H. Stalz, W. Stelzer, F. Hulsbergen, H. de Groot, K. Gerwert, J. Reed, D. Langosch, *De novo* design of conformationally flexible transmembrane peptides driving membrane fusion, Proc. Natl. Acad. Sci. U. S. A. 101 (2004) 14776–14781.
[8] P. Agrawal, S. Kiihne, J. Hollander, D. Langosch, H. de Groot, 13C and 15N NMR evidence for peripheral intercalation of uniformly labeled fusogenic peptides incorporated in a biomimetic membrane, Biochim. Biophys. Acta (BBA) - Biomembranes 1768 (2007) 3020–3028.
[9] B.C. Poschner, S. Quint, M. Hofmann, D. Langosch, Sequence-specific conformational dynamics of model transmembrane domains determines their membrane fusogenic function, J. Mol. Biol. 386 (2009) 733–741.
[10] S.J. Opella, NMR and membrane proteins, Nat. Struct. Biol. 4 (1997) 845–848.
[11] K.A.H. Wildman, D.K. Lee, A. Ramamoorthy, Mechanism of lipid bilayer disruption by the human antimicrobial peptide, LL-37, Biochemistry 42 (2003) 6545–6558.
[12] A. Ramamoorthy, F.M. Marassi, M. Zasloff, S.J. Opella, 3-Dimensional solid-state NMR-spectroscopy of a peptide oriented in membrane bilayers, J. Biomol. NMR 6 (1995) 329–334.
[13] F.M. Marassi, A. Ramamoorthy, S.J. Opella, Complete resolution of the solid-state NMR spectrum of a uniformly N-15-labeled membrane protein in phospholipid bilayers, Proc. Natl. Acad. Sci. U. S. A. 94 (1997) 8551–8556.
[14] B. Bechinger, Solid-state NMR investigations of interaction contributions that determine the alignment of helical polypeptides in biological membranes, FEBS Lett. 504 (2001) 161–165.
[15] B. Bechinger, R. Kinder, M. Helmle, T.C.B. Vogt, U. Harzer, S. Schinzel, Peptide structural analysis by solid-state NMR spectroscopy, Biopolymers - Peptide Science 51 (1999) 174–190.
[16] K.J. Hallock, K. Henzler Wildman, D.K. Lee, A. Ramamoorthy, An innovative procedure using a sublimable solid to align lipid bilayers for solid-state NMR studies, Biophys. J. 82 (2002) 2499–2503.
[17] D.P. Siegel, The modified stalk mechanism of lamellar/inverted phase transitions and its implications for membrane fusion, Biophys. J. 76 (1999) 291–313.
[18] P. Agrawal, S. Kiihne, J. Hollander, F. Hulsbergen, M. Hofmann, D. Langosch, H. de Groot, Solid state NMR investigation of the interaction between biomimetic lipid bilayers and a *de novo* designed fusogenic peptide, ChemBioChem 8 (2007) 493–496.
[19] J. Ollesch, B.C. Poschner, J. Nikolaus, M.W. Hofmann, A. Herrmann, K. Gerwert, D. Langosch, Secondary structure and distribution of fusogenic LV-peptides in lipid membranes, Europ. Biophys. J. 37 (2008) 435–445.
[20] P. Agrawal, M. Hofmann, N. Meeuwenoord, D. Filippov, H. Stalz, F. Hulsbergen, D. Langosch, H. Overkleeft, H. de Groot, Solid-phase synthesis and purification of a set of uniformly ^{13}C, ^{15}N labelled *de novo* designed membrane fusogenic peptides, J. Pept. Sci. 13 (2007) 75–80.
[21] D. Langosch, J.M. Crane, B. Brosig, A. Hellwig, L.K. Tamm, J. Reed, Peptide mimics of SNARE transmembrane segments drive membrane fusion depending on their conformational plasticity, J. Mol. Biol. 311 (2001) 709–721.
[22] M. Rance, R.A. Byrd, Obtaining high-fidelity spin-1/2 powder spectra in anisotropic media-phase-cycled Hahn echo spectroscopy, J. Magn. Reson. 52 (1983) 221–240.
[23] J.W. Deutsch, R.B. Kelly, Lipids of synaptic vesicles: relevance to the mechanism of membrane fusion, Biochemistry 20 (1981) 378–385.
[24] S. Takamori, M. Holt, K. Stenius, E.A. Lemke, M. Gronborg, D. Riedel, H. Urlaub, S. Schenck, B. Brugger, P. Ringler, S.A. Muller, B. Rammner, F. Grater, J.S. Hub, B.L. De Groot, G. Mieskes, Y. Moriyama, J. Klingauf, H. Grubmuller, J. Heuser, F. Wieland, R. Jahn, Molecular anatomy of a trafficking organelle, Cell 127 (2006) 831–846.
[25] J.J. Buffy, M.J. McCormick, S. Wi, A. Waring, R.I. Lehrer, M. Hong, Solid-state NMR investigation of the selective perturbation of lipid bilayers by the cyclic antimicrobial peptide RTD-1, Biochemistry 43 (2004) 9800–9812.
[26] J.M. Pearce, R.A. Komoroski, Resolution of phospholipid molecular species by 31P NMR, Magn. Reson. Med. 29 (1993) 724–731.
[27] K.J. Hallock, D.K. Lee, A. Ramamoorthy, MSI-78, an analogue of the magainin antimicrobial peptides, disrupts lipid bilayer structure via positive curvature strain, Biophys. J. 84 (2003) 3052–3060.
[28] D.B. Fenske, H.C. Jarrell, P-31 2-dimensional solid-state exchange NMR—application to model membrane and biological-systems, Biophys. J. 59 (1991) 55–69.
[29] F. Picard, M.J. Paquet, E.J. Dufourc, M. Auger, Measurement of the lateral diffusion of dipalmitoylphosphatidylcholine adsorbed on silica beads in the absence and presence of melittin: a P-31 two-dimensional exchange solid-state NMR study, Biophys. J. 74 (1998) 857–868.
[30] L. Chernomordik, Non-bilayer lipids and biological fusion intermediates, Chem. Phys. Lipids 81 (1996) 203–213.
[31] S.J. Marrink, A.E. Mark, The mechanism of vesicle fusion as revealed by molecular dynamics simulations, J. Am. Chem. Soc. 125 (2003) 11144–11145.
[32] V. Knecht, S.J. Marrink, Molecular dynamics simulations of lipid vesicle fusion in atomic detail, Biophys. J. 92 (2007) 4254–4261.
[33] K. Katsov, M. Müller, M. Schick, Field theoretic study of bilayer membrane fusion: II. Mechanism of a Stalk–Hole complex, Biophys. J. 90 (2006) 915–926.
[34] S.G. Ostrowski, C.T. Van Bell, N. Winograd, A.G. Ewing, Mass spectrometric imaging of highly curved membranes during tetrahymena mating, Science 305 (2004) 71–73.